




# Orbital-angular-momentum-resolved diagnostics for tracking internal phase evolution in multi-bound solitons

YUWEI ZHAO,<sup>1</sup> JINTAO FAN,<sup>1,2,3</sup> YOUJIAN SONG,<sup>1,4</sup>  AND MINGLIE HU<sup>1,5</sup> 

<sup>1</sup>Ultrafast Laser Laboratory, Key Laboratory of Opto-electronic Information Science and Technology of Ministry of Education, School of Precision Instruments and Opto-electronics Engineering, Tianjin University, 300072 Tianjin, China

<sup>2</sup>Institut für Quantenoptik, Leibniz Universität Hannover, Welfengarten 1, 30167 Hannover, Germany

<sup>3</sup>Cluster of Excellence PhoenixD (Photonics, Optics, and Engineering-Innovation Across Disciplines), 30167 Hannover, Germany

<sup>4</sup>yjsong@tju.edu.cn

<sup>5</sup>huminglie@tju.edu.cn

**Abstract:** The generation of multi-bound solitons is a fascinating subject of investigation in many conservative and dissipative systems, such as photonics, fluid mechanics, Bose-Einstein condensates, and so on. In this study, we demonstrate the successful extraction of phase dynamics between solitons in bound multiple solitons with up to seven constituents in a mode-locked Er laser system. By mapping the internal phase motions of multi-bound solitons to the spatial phase movement of cylindrical vector beams using orbital angular momentum (OAM)-based diagnostics, different categories of internal pulsations are revealed. We show that bound state of four solitons exhibits linear drifting relative phase evolution dynamics; while for bound multiple solitons with constituents from five to seven pulses, stationary relative phase dynamics are observed. These findings highlight the possibility of the OAM-based method access to the internal motion of multi-soliton molecules with more freedom of degrees and fuel the analogy with research on chemistry molecule complex.

© 2021 Optical Society of America under the terms of the [OSA Open Access Publishing Agreement](#)

## 1. Introduction

Passively mode-locked fiber laser has become a versatile and reliable platform for exploring diverse nonlinear dynamics in a dissipative system [1]. Besides single soliton generation, multiple soliton states have also been observed in various fiber laser configurations [2]. Both states can be described by nonlinear Schrödinger-Ginzburg-Landau equation and coupled nonlinear Schrödinger equations [3,4]. For the practical application field, lasers operating at multiple soliton states could increase the capacity of communication and optical storage [5]. For the fundamental scientific aspect, exploring the soliton evolution within multi-soliton states is of great significance to understand the general dynamics of complex systems [6,7]. Therefore, it is an urgent demand for investigating the properties and dynamics of multi-soliton states in a laser system at a fundamental level.

In last decade, numerical simulations have revealed the formation and evolution of internal motions within multi-soliton states in various fiber lasers [8,9]. Nevertheless, at the beginning, the time averaging measurement conducted by spectrometer and autocorrelator seriously limit the direct monitoring of dynamical evolution process [2]. Fortunately, the emergence of real time dispersive Fourier transform (DFT) technique greatly pushes the frontier of deep understanding of multiple solitons formation by mapping the optical spectrum of the output pulses onto temporal waveform through group velocity dispersion. To date, by controlling the nonlinear loss and pump

power of laser systems, numerous multi-soliton patterns have been observed, such as soliton rains [10], soliton crystals [11], soliton explosions [12], soliton collisions [13,14], and harmonic mode-locking [15], etc. Among them, bound state stands out due to its unique pulse interaction properties and fixed discrete pulse separations. Bound solitons, which are in analogy with matter molecular, once formed, are relative stable and will propagate almost indefinitely in the laser cavity. The most common case of bound solitons is bi-soliton. Two independent studies in 2017 have been conducted to monitor the real time evolution of bi-soliton in a laser cavity using DFT technique, which opens a new door for investigating the complex phase dynamics within soliton molecules [16,17]. Since then, the research related to bi-soliton has experienced an explosive development. Abundant formation and interaction dynamics within bi-soliton have been revealed in a large number of laser systems based on different mode locking mechanism [18–21]. To further comprehend the physical dynamics of soliton macromolecules, it's worthwhile to study bound solitons with more constituents. Generally, the formation of multi-soliton modes can be mainly traced back to two aspects: peak-power-limiting effect and gain bandwidth limited pulse splitting [22,23]. Internal dynamics within 1 + 2 or 2 + 2 soliton molecular complex (SMC) and tri-bounded solitons have been characterized with DFT technique [16,24,25]. Although the spectral resolution of the DFT technique can be down to one of ten nanometers [17], when the constituents of the bound solitons further increase, the application of such technique do have limitations due to the current recording features of fast electronics. The observation time frame of DFT technique is limited to hundreds of micro seconds mainly confined by the storage capability of the real time oscilloscopes. Therefore, although multi-bound soliton states have already been observed in various laser systems [26–28], the experimental characterization of internal dynamics of bounded solitons with more constituents remains a practical challenge.

To address this issue, in this paper, we report an orbital angular momentum (OAM)-based diagnostic to track phase motions in femtosecond multi-bound solitons. Phase dynamics between every two solitons can be successfully extracted in bound solitons with up to seven constituents. Two different categories of multi-bound soliton dynamics are highlighted here. The first one is a slightly linear drifting relative phase motion soliton quadruplet. The second two mainly consists of stationary multi-bound soliton with more than four constituents. All these findings can provide new insights into internal phase dynamics of bound solitons with more freedom of degrees and highlight the possible applications for high capacity data storage and telecommunication.

## 2. Experimental setup

The all-polarization maintaining (PM) nonlinear amplifying loop mirror (NALM) mode-locked fiber laser that we build to study multiple solitons is similar to our previous reported one in [29]. The laser parameters are shown as follows: 0.74-m long Erbium-doped gain fiber (EDF) (Liekki, Er80-4/125-HD-PM) is used, the group velocity dispersion (GVD) of which is  $-30.58$  ps/nm/km at 1550 nm, 1.57 m long single-mode fiber with the GVD of 16 ps/nm/km from the pigtail of components, a wavelength-division multiplexer (WDM) for pump incident, a fiber-pigtailed polarization beam splitter, a fiber based collimator and free-space optical components. All the fiber is polarization maintaining. The gain fiber is pumped by a 680mW single mode laser diode operating at 976 nm. The calculated net dispersion of the cavity is about  $-0.0032$  ps<sup>2</sup>, which is much closer to zero-dispersion regime than that in [29]. The total cavity length is around 2.48 m, and the corresponding fundamental repetition rate is  $\sim 84$  MHz.

Through simultaneously controlling the pump power and adjusting the arrangement of waveplates inside the laser cavity, single pulse, bound doublet and triplet operation can be readily obtained. What's more, bound solitons composed of a large population of optical solitons can also be formed in the same way. As shown in Fig. 1, the output of the laser is split into two arms by a beam splitter (BS). The spectrum analyzer is used to record the optical spectrum of the multi-bound solitons, while the OAM system is utilized to detect the relative phase information

within multi-bound solitons. Previously, we have successfully characterized two different kinds of soliton molecular phase properties in soliton pairs and soliton triplet, based on OAM-resolved method [29]. Notice that the proposed method relies on the temporal overlap between solitons. Consequently, despite the fact that multiple solitons possess more degrees of freedom compared to bi- or tri-solitons, our technique still has the capability to reveal the phase dynamics in bound solitons with more constituents by finely tuning the time delay. Finally, we utilize a commercially available CCD (Bobcat-320, Xenics) to record a sequence of images at a capturing rate of one frame per ten milliseconds for tracking the long-term variation of the relative phase difference among the multi-soliton molecules. The exposure time for obtaining each beam profile is set to be as short as 5.6  $\mu\text{s}$ . More detailed description about experimental setup and working principle of the OAM-resolved method can be found in [29].

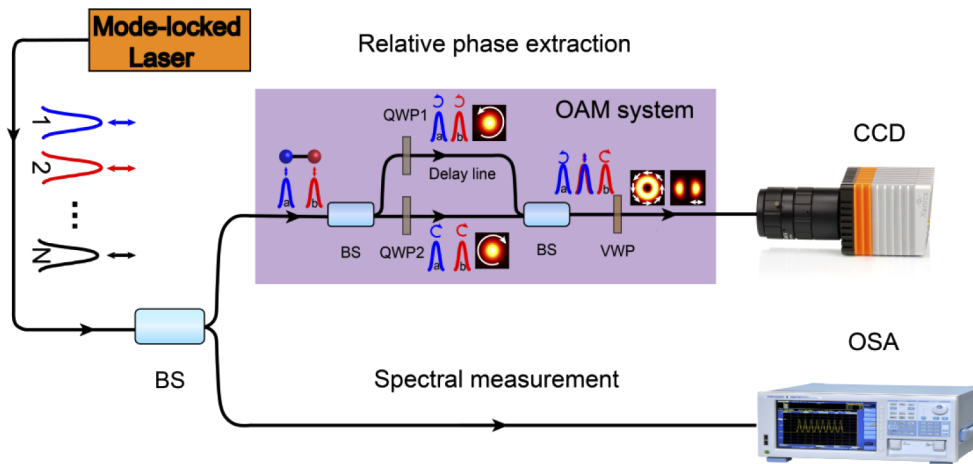


**Fig. 1.** Experimental setup. Mode-locked laser, all-polarization maintaining (PM) nonlinear amplifying loop mirror (NALM) mode-locked Er-doped fiber laser; BS, beam splitter; OAM-system, orbital-angular-momentum resolved system. OSA, optical spectrum analyzer.

### 3. Results and discussion

#### 3.1. Numerical simulation

Initially, we conduct a simple simulation to reveal the relationship between the internal phase dynamics and the spectral features of the multi-bound solitons. Guided by [17], the quadruplet soliton molecule consists of four bound solitons evolving with cavity roundtrip time is shown here. The temporal separation and relative phase are marked as  $\tau$  and  $\phi$ , respectively. Let us sum four identical Gaussian pulses with fixed temporal separations of 990 fs [Fig. 2(a)],  $s(t) = \psi[t - \frac{3\tau}{2}] + \psi[t - \frac{\tau}{2}]e^{-i\phi} + \psi[t + \frac{\tau}{2}]e^{-i2\phi} + \psi[t + \frac{3\tau}{2}]e^{-i3\phi}$ , where  $\psi$  is a Gaussian envelope and  $t$  is the time in the commoving reference frame. The intensity can be calculated by  $I(w) = |S(w)|^2$ . Considering  $\phi = -kz + \phi_0$ , as displayed in Fig. 2(b), we could achieve a slowly linearly evolving bound soliton states with four solitons. This will result in a high contrast spectral fringe pattern with a slightly drifting away behavior, as shown in Fig. 2(c). The simulation results shown here coincide well with the extracted phase dynamical evolution characteristic via OAM-method.

#### 3.2. Preliminary experiment

In principle, arbitrary two solitons in one bound packet are selected and overlapped in OAM system. As mentioned before, the method here strongly depends on the temporal delay provided

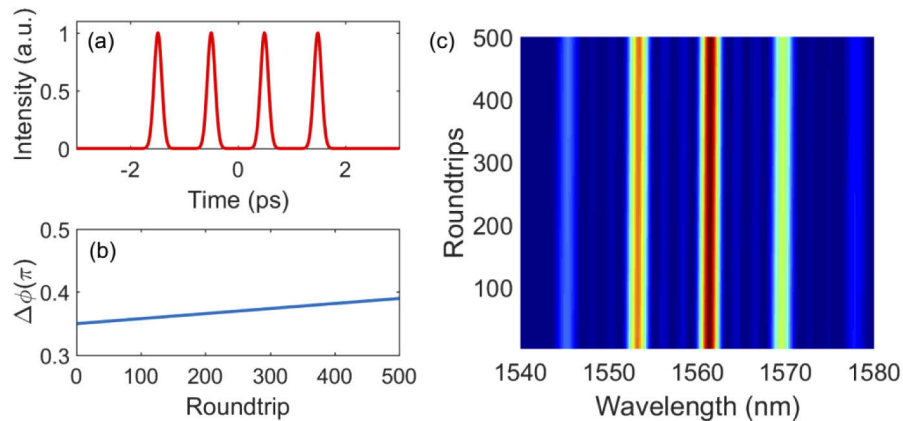


**Fig. 2.** (a) and (b) Temporal property and relative phase of simulated bound soliton with four constituents; (c) Spectral dynamics over 500 round trips in terms of linear relative phase evolution.

by the translation stage. Therefore, high precision differential beam path tuning is essential. An automatically translation stage (MT1-Z8, Thorlabs) with step size of 200 nm is used here. The differential arm length fluctuation will transfer to phase fluctuation through  $\theta(\Delta L) = \pi\nu\Delta L/c$ , where  $\nu$  is the central frequency of the laser pulse,  $\Delta L$  is beam path difference between two arms of the Mach-Zehnder-like interferometer (MZI). We conduct an experiment in advance to show the beam path tuning precision of our system. The mode-locked laser has been set as a single pulse operation state in this case. Each soliton beam is splitted, and re-combined after propagation in the MZI with equal arm length. The translation stage is moved step by step. A comparison between the calculated phase difference and the retrieved one is presented in Fig. 3. Obviously, high precision differential beam path tuning is realized. In additional, the resolution of the OAM-based technique is determined by the angle resolution for the extraction of rotation direction of the interferometric pattern. By comparing the retrieved angles from the computer-generated lobe patterns with stepped increasing rotation angle (not shown here), we address here the angle resolution for extracting the rotation direction of an interferometric pattern is  $\sim 0.001\pi$  rad, which is enough to identify the internal phase dynamical evolution within bound solitons.

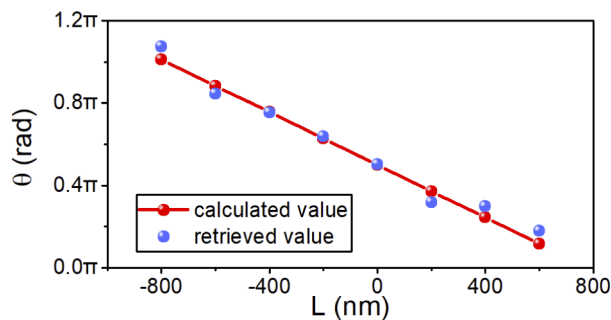


**Fig. 3.** Comparison between the retrieved phase difference and calculated value at various MZI arm length differences.

### 3.3. Quadruplet soliton molecule with monotonically evolving phase

The output pulse states present highly dependence with respect to the pumping power and polarization states inside laser cavity. We start the laser at a pump power of 545 mW, where a four pulses state is obtained. Meanwhile, the angles of the polarization waveplates are carefully tuned to change the pulse interaction. Pulse self-assembly occurs during this process, forming quadruplet soliton molecule, consisting of four identical bound solitons. The averaged spectrum in linear scale is shown in Fig. 4(a), the close up 30-nm spectrum in logarithmic coordinate is plotted in inset. As can be seen, the typical Kelly sidebands are not formed. This can be ascribed by the fact that the dispersion of the total cavity is near zero, and hence the laser operated at dispersion managed soliton regime. To this end, the chirp stretches the pulse within the cavity in each roundtrip, profiting the interaction among multiple solitons [23]. The corresponding autocorrelation trace shown in Fig. 4(b) reveals the identical separation within each neighboring soliton and also the same peak intensity of each soliton. The readout time separation among the solitons is 990 fs, which matches well with the spectral modulation period of 2 nm in Fig. 4(a). Figure 4(c) shows the measured spectral evolution over 10 min by using the optical spectrum analyzer. The acquisition time for each spectrum is 8 s. The unchanged 2D contour plot with two bright and two dark fringes imply the good stability of the quadruplet soliton molecule. Nevertheless, confined by the long integration time, the 2D contour plots obtained by an optical spectral analyzer fail to unveil the evolving relative phase over time. To gain insight into transient dynamics, we retrieve the relative phases within the quadruplet using OAM-resolved method. Hereafter, we label the solitons within quadruplet as 1, 2, 3, 4 and define the variables as:  $\Delta\phi_{ij}$  ( $i, j=1, 2, 3, 4$ ) and  $\theta_{ij}$  ( $i, j=1, 2, 3, 4$ ) represent the relative phases between the two solitons of the quadruplet and the corresponding retrieved relative phases based on OAM-resolved method, respectively. As a simple example,  $\Delta\phi_{14}$  and  $\theta_{14}$  describe the relative phase and the retrieved relative phase between the leading soliton ( $i=1$ ) and the tailing soliton ( $j=4$ ) within quadruplet soliton molecule. Figure 4(d) presents the relative phases evolution within the quadruplet soliton molecule over 2 s based on the OAM-resolved method. The red curve corresponds to the superposed relative phase variation of  $\theta_{12}$ ,  $\theta_{23}$ , and  $\theta_{34}$ , the purple curve shows the variation of  $\theta_{14}$ . In these two cases, the slopes are quite similar when linearly fitting the variations of relative phase motions, confirming the relationship of  $\Delta\phi_{12}+\Delta\phi_{23}+\Delta\phi_{34}=\Delta\phi_{14}$ . This further validates the consistency of our phase retrieval. Similar to the dynamics observed in soliton

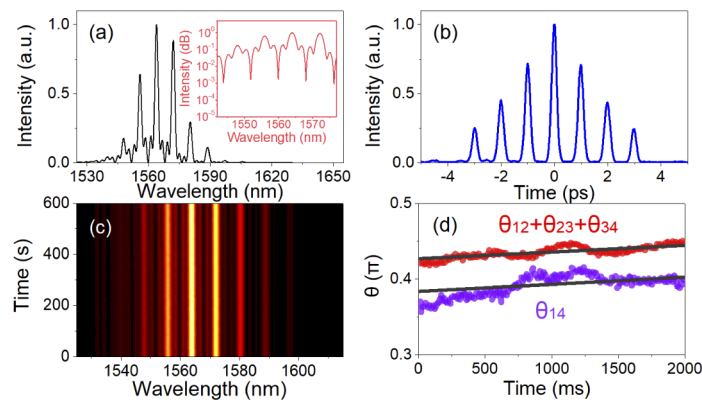


**Fig. 4.** Internal phase dynamics within a quadruplet soliton molecule. (a) Spectrum of the quadruplet soliton molecule, the inset is the close-up spectrum under logarithmic coordinate. (b) Autocorrelation trace of the quadruplet soliton molecule, (c) spectral intensity variation during 10 min, (d) relative phase evolution of  $\theta_{12}+\theta_{23}+\theta_{34}$  and  $\theta_{14}$  based on the OAM-resolved method.

triplet, a slowly linearly evolving motion between the tailing soliton and the leading soliton is revealed [30].

### 3.4. Multi-bound soliton with stationary phase

We now turn to multi-bound solitons with even more constituents. Generally, the polarization adjustment will influence the pulse evolution dynamics per roundtrip, resulting in different operation states of the output. Hence, the pump power is maintained at 560 mW, with the appropriate waveplates arrangement, multi-soliton molecules constituted by five (six, seven) dispersion managed solitons can be created. In each case, the soliton constituents are equally spaced with identical duration and exist indefinitely in time as a bounded packet. Figure 5 summarizes the laser output performance of multi-solitons in different states. Obviously, with the increase of intramolecular soliton populations, the temporal separation between two neighboring solitons increases from 920 fs to 975 fs, which can also be reflected by the decreasing of spectral modulation periods. Furthermore, the pulses' amplitudes increase with the number of bound solitons, thus the strength of the molecules against perturbations grows up. Remarkably the multi-soliton state consisting of equally spaced solitons separated by <1 ps that is the shortest separation obtained in multi-bound soliton cases. By extension of the terminology suggested for soliton pair molecules, the proposed terminology for the currently reported multiple solitons can be referred to be "ground-state bound multi-solitons".

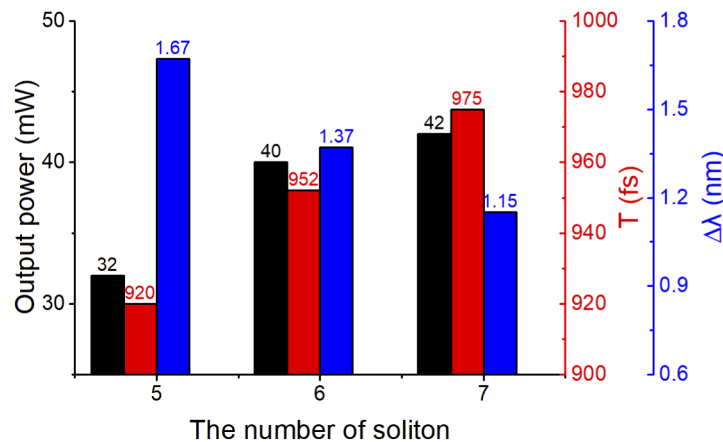


**Fig. 5.** The output powers, soliton separations, and spectral modulation periods of five, six, and seven soliton molecules.

The averaged full optical spectrum in linear scale and close-up spectrum in 25 nm (logarithmic scale) for soliton molecules constituted by five, six, seven dispersion managed solitons are shown in Figs. 6(a), 6(c) and 6(e), respectively. The number of solitons can be reflected by the interference structure of the spectrum combined with the number of dips located on the spectrum. It is evident from close up spectrum that spectral interference all present high contrast fringes, indicating stable binding soliton interaction. Furthermore, we investigate the relative phase evolution among the bound multiple solitons. As displayed in Figs. 6(b), 6(d) and 6(f), we find that the relative phases between two neighboring solitons within soliton molecule in the present case are kept nearly constant during the evolution process. We also record the relative phase evolution between other combinations of two solitons beyond the neighboring one in the bound-multi soliton wave packet, not shown here. Relative phase motions between arbitrary two solitons can be readily obtained by shifting the time delay using the translation stage with the aid of autocorrelator as monitor. No obvious relative phase motion in all conditions

except for some vibrations probably caused by the environmental disturbance. In terms of the consistency relationship of  $\sum_{i=1}^k \Delta\phi_{i,i+1} = \Delta\phi_{1,k}$  ( $k = 5, 6, 7$ ), we can conclude that the pulses within the multi-soliton states are mainly phase-locked with an identical intramolecular separation. This demonstrates again the fact that a static soliton molecule with five (six, seven) constituents is formed. We interpret our results to be an extension of soliton pairs. The single soliton explodes to several soliton constituents, and then several solitons co-propagate in the laser cavity, repel and attract each other until bound solitons with fixed separations and locked relative phases are obtained. We present that soliton molecules can form various bounds related to the temporal separation between soliton constituents and also the single soliton amplitude. Even the internal degrees of freedom of multi-soliton molecules increase considerably, the intrinsic formation mechanism can still lead to a stable state, which resembles the formation of large chemical molecular structures.

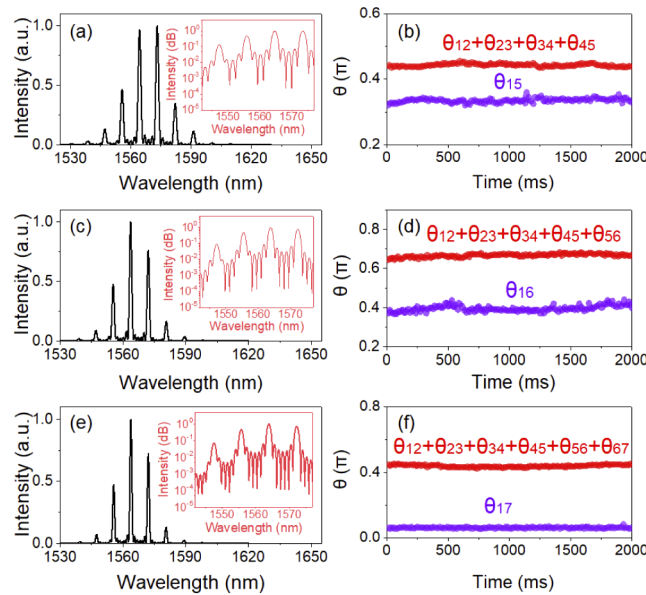


**Fig. 6.** Internal phase evolution within multi-soliton molecules constituted by five, six, and seven solitons. (a), (c) and (e) The linear spectrum of five, six, and seven multi-bound soliton states. The insets are the corresponding 25 nm close-up spectrum under logarithmic coordinate. (b), (d) and (f) The internal phase evolution within five, six, and seven multi-bound soliton states.

#### 4. Conclusion

To conclude, we successfully resolve the relative phase evolution of multi-bound solitons with larger number of constituents using the OAM-resolved method. Beyond bi-soliton and tri-soliton molecules, multi-soliton molecules have more degrees of freedom in terms of temporal separation and relative phase. Generally, the characterization of such tightly bound multi-soliton patterns remains challenging. By mapping the internal temporal phase to the interference pattern of two vortices, our method presents a simple and suitable way for visually monitoring the relative phase changes within soliton molecular complex with more constituents. Going forward, a high-performance CCD with exposure time down to 1 ns is utilized, our method possesses the potential to be a real time diagnostic, thus probing the transient buildup process of various soliton states, e.g., multi-bound solitons, bidirectional solitons, vector solitons. From the dynamical

point of view, the formation of soliton molecules with large number of solitons could spread new perspectives into supramolecular chemistry. Beneficial from more degrees of freedom in one bound packet, the present multi-bound solitons could find potential applications for high capacity optical bit storage and manipulation of nanoparticles.

**Funding.** National Natural Science Foundation of China (618278221, 61975144); the European Union's Horizon 2020 Research and Innovation Programme under the Marie Skłodowska Curie grant (713694); the State Key Laboratory of Advanced Optical Communication Systems and Networks, Shanghai Jiao Tong University, China (2020GZKF011).

**Disclosures.** The authors declare no conflicts of interest.

**Data availability.** Data underlying the results presented in this paper are not publicly available at this time but may be obtained from the authors upon reasonable request.

## References

1. L. Gui, P. Wang, Y. Ding, K. Zhao, C. Bao, X. Xiao, and C. Yang, "Soliton molecules and multisoliton states in ultrafast fibre lasers: intrinsic complexes in dissipative systems," *Appl. Sci.* **8**(2), 201 (2018).
2. P. Grelu and N. Akhmediev, "Dissipative solitons for mode-locked lasers," *Nat. Photonics* **6**(2), 84–92 (2012).
3. B. A. Malomed, "Bound solitons in the nonlinear Schrödinger–Ginzburg–Landau equation," *Phys. Rev. A* **44**(10), 6954–6957 (1991).
4. B. A. Malomed, "Bound solitons in coupled nonlinear Schrödinger equations," *Phys. Rev. A* **45**(12), R8321–R8323 (1992).
5. M. Pang, W. He, X. Jiang, and P. S. J. Russell, "All-optical bit storage in a fibre laser by optomechanically bound states of solitons," *Nat. Photonics* **10**(7), 454–458 (2016).
6. F. M. Mitschke and L. F. Mollenauer, "Experimental observation of interaction forces between solitons in optical fibers," *Opt. Lett.* **12**(5), 355–357 (1987).
7. R. Weill, A. Bekker, V. Smulakovsky, B. Fischer, and O. Gat, "Noise-mediated Casimir-like pulse interaction mechanism in lasers," *Optica* **3**(2), 189–192 (2016).
8. V. Voropaev, A. Donodin, A. Voronets, D. Vlasov, V. Lazarev, M. Tarabrin, and A. Krylov, "Generation of multi-solitons and noise-like pulses in a high-powered thulium-doped all-fiber ring oscillator," *Sci. Rep.* **9**(1), 18369 (2019).
9. P. Grelu and J. M. Soto-Crespo, "Multisoliton states and pulse fragmentation in a passively mode-locked fibre laser," *J. Opt. B Quantum Semiclass. Opt.* **6**(5), S271–S278 (2004).
10. S. Chouli and P. Grelu, "Rains of solitons in a fiber laser," *Opt. Express* **17**(14), 11776–11781 (2009).
11. A. Andrianov and A. Kim, "Extremely elastic soliton crystals generated in a passively mode-locked tunable high-repetition-rate fiber laser", arXiv:1905.03129, 2019, [online] Available: <https://arxiv.org/abs/1905.03129>.
12. J. Peng and H. Zeng, "Soliton collision induced explosions in a mode-locked fibre laser," *Commun. Phys.* **2**(1), 34 (2019).
13. J. Peng, N. Tarasov, S. Sugavanam, and D. Churkin, "Rogue waves generation via nonlinear soliton collision in multiple-soliton state of a mode-locked fiber laser," *Opt. Express* **24**(19), 21256–21263 (2016).
14. M. Olivier, V. Roy, M. Piché, and F. Babin, "Pulse collisions in the stretched-pulse fiber laser," *Opt. Lett.* **29**(13), 1461–1463 (2004).
15. F. Amrani, A. Haboucha, M. Salhi, H. Leblond, A. Komarov, P. Grelu, and F. Sanchez, "Passively mode-locked erbium-doped double-clad fiber laser operating at the 322nd harmonic," *Opt. Lett.* **34**(14), 2120–2122 (2009).
16. G. Herink, F. Kurtz, B. Jalali, D. R. Solli, and C. Ropers, "Real-time spectral interferometry probes the internal dynamics of femtosecond soliton molecules," *Science* **356**(6333), 50–54 (2017).
17. K. Krupa, K. Nithyanandan, U. Andral, P. Tchofo-Dinda, and P. Grelu, "Real-time observation of internal motion within ultrafast dissipative optical soliton molecules," *Phys. Rev. Lett.* **118**(24), 243901 (2017).
18. P. Ryczkowski, M. Närhi, C. Billet, J.-M. Merolla, G. Genty, and J. M. Dudley, "Real-time full-field characterization of transient dissipative soliton dynamics in a mode-locked laser," *Nat. Photonics* **12**(4), 221–227 (2018).
19. M. Liu, H. Li, A.-P. Luo, H. Cui, W. Xu, and Z. Luo, "Real-time visualization of soliton molecules with evolving behavior in an ultrafast fiber laser," *J. Opt.* **20**(3), 034010 (2018).
20. X. Liu, X. Yao, and Y. Cui, "Real-time observation of the buildup of soliton molecules," *Phys. Rev. Lett.* **121**(2), 023905 (2018).
21. J. Peng and H. Zeng, "Build-up of dissipative optical soliton molecules via diverse soliton interactions," *Laser Photonics Rev.* **12**(8), 1800009 (2018).
22. D. Y. Tang, L. M. Zhao, B. Zhao, and A. Q. Liu, "Mechanism of multisoliton formation and soliton energy quantization in passively mode-locked fiber lasers," *Phys. Rev. A* **72**(4), 043816 (2005).
23. X. Liu, "Interaction and motion of solitons in passively-mode-locked fiber lasers," *Phys. Rev. A* **84**(5), 053828 (2011).
24. Z. Q. Wang, K. Nithyanandan, and A. Coillet, "Optical soliton molecular complexes in a passively mode-locked fibre laser," *Nat. Commun.* **10**(1), 830 (2019).
25. A. Kokhanovskiy, E. Kuprikov, and S. Kobtsev, "Single- and multi-soliton generation in figure-eight mode-locked fibre laser with two active media," *Opt. Laser Technol.* **131**, 106422 (2020).



26. D. Y. Tang, L. M. Zhao, and B. Zhao, "Multipulse bound solitons with fixed pulse separations formed by direct soliton interaction," *Appl. Phys. B* **80**(2), 239–242 (2005).
27. D. Y. Tang, W. S. Man, H. Y. Tam, and P. D. Drummond, "Observation of bound states of solitons in a passively mode-locked fiber laser," *Phys. Rev. A* **64**(3), 033814 (2001).
28. Y. F. Song, H. Zhang, L. M. Zhao, D. Y. Shen, and D. Y. Tang, "Coexistence and interaction of vector and bound vector solitons in a dispersion-managed fiber laser mode locked by graphene," *Opt. Express* **24**(2), 1814–1822 (2016).
29. Y. Zhao, J. Fan, Y. Song, U. Morgner, and M. Hu, "Extraction of internal phase motions in femtosecond soliton molecules using an orbital-angular-momentum-resolved method," *Photonics Res.* **8**(10), 1580–1585 (2020).
30. Y. Luo, R. Xia, P. P. Shum, W. Ni, Y. Liu, H. Q. Lam, Q. Sun, X. Tang, and L. Zhao, "Real-time dynamics of soliton triplets in fiber lasers," *Photonics Res.* **8**(6), 884–891 (2020).